

AN EXPERIMENTAL AND NUMERICAL STUDY OF FLOW PATTERNS AT A 30 DEGREE WATER INTAKE FROM TRAPEZOIDAL AND RECTANGULAR CHANNELS*

M.KARAMI MOGHADAM^{1, **}, M. SHAFAI BAJESTAN², H. SEDGHI³ AND M. SEYEDIAN⁴

¹Dept. of Agriculture, Payame Noor University, Tehran, I. R. of Iran

Email: m_karami_mo@yahoo.com

²College of Water Science and Engineering, Shahid Chamran University, Ahwaz, I. R. of Iran

³Dept. of Water Engineering, Science and Research Branch, Islamic Azad University (IAU), Tehran, I. R. of Iran

⁴Agriculture Faculty, Gonbad Kavous University, I. R. of Iran

Abstract– Knowing flow pattern, especially stream tube dimensions at the vicinity of a lateral intake is important to study flow discharge and sediment rate entering to the intake as well as to better design a measure for controlling sediment entry into the intake. Previous studies have been focused on intake from rectangular channels. In the present study, however, different experimental tests were carried out at a 30 degree water intake installed at bank of a trapezoidal channel to measure the three components of flow velocities; these data were then applied to calibrate the numerical SSIIM2 model; by running the SSIIM2 model for different flow conditions, more data were obtained. From the analysis of both experimental and numerical data the flow patterns upstream of intake were plotted and the stream tube dimensions were obtained for all flow conditions. It was found that the dividing stream width for intake from trapezoidal canal at the bottom is less than it is for intake from rectangular canal for the same flow conditions; the width at any elevation was found to depend directly on the diversion flow ratio. Relations for predicting dividing stream width as a function of diversion flow ratio have been presented for intake from both rectangular and trapezoidal cross sections. Also, computed secondary current strength at the intake entrance, which is an effective parameter in transporting sediment to the intake, showed that it is a function of flow diversion ratio and for intake from trapezoidal channel it is less than from rectangular channel.

Keywords– Dividing stream width, trapezoidal channel, secondary current

1. INTRODUCTION

The study of flow patterns in front of intake has attracted the attention of researchers during the past decades to explore the mechanism of flow and sediment entry to the intake. Taylor [1] was the first to study the flow in the 90 degree intake and proposed a graphical method for determining the 2 dimensional flow patterns. Thomson [2], Tanaka [3], Murota [4], Grace and Priest [5], Law and Reynolds [6], Hager [7, 8] and Neary and Odgaard [9] also studied the 2 dimensional flow patterns in front of rectangular intake. Neary et al. [10] was a pioneer who conducted a 3 dimensional numerical model at a lateral intake from a rectangular canal and plotted the resulting flow patterns as shown in Fig.1. Among the different flow zones shown in Fig.1, the dividing separation surface is the interest of the present paper. When approaching flow to the intake it is accelerated laterally due to the suction pressure at the end of the intake. The acceleration divides the flow into two parts, one entering the inside of the intake, and the other continues to the downstream of the channel. The former is shown in Fig.1 by a surface called the Dividing

*Received by the editors January 20, 2011; Accepted January 1, 2014.

**Corresponding author

Stream Surface (DSS) or stream tube. As seen in Fig.1 (section 2-2), the diversion flow width at the bed (B_b) is greater than that in the surface (B_s), this is because the bottom layer which has lower velocity can be more affected by the intake suction than the surface layer with higher flow velocity. Since the water and sediment within the DSS are entering the intake, predicting DSS dimensions can determine the rate of flow and sediment discharge to the branch channel.

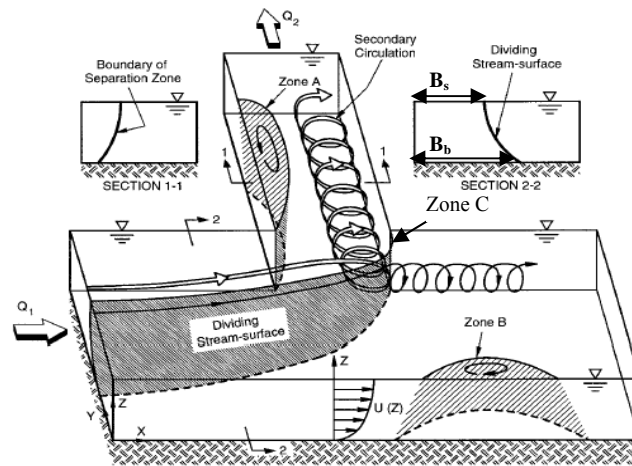


Fig. 1. The flow pattern in the intake entrance [10]

Barkdoll [11] showed in his researches on the lateral intake, which are carried out in straight path with 90 degree intake angle, that the diversion flow ratio has the greatest effect on the sediment delivery ratio. Weber et al. [12] performed an extensive experimental study of combining flows in a 90° open channel for the purpose of providing a very broad data set comprising three velocity components, turbulence stresses, and water surface mappings. Huang et al. [13] performed a comprehensive numerical study using the 3D turbulence models, and validated the model using the data applied by Weber et al. [12]. The initiation of sediment motion in fixed bed and V-shaped bottom channels was investigated by Mohammadi [14]. The results show that the effect of cross sectional shape on sediment threshold in fixed bed channels should be examined. Using experimental data and comparing it with a numerical model which solves the standard 3-dimensional equations RANS for unsteady turbulent flows, Ramamurthy et al. [15] have shown that at the dividing flows, the mean exit angle of the streamlines for flow entering the branch larger at the surface compared to the exit angles of the streamlines located at the bottom. A three-dimensional turbulent flow field in a 180 degree channel bend with a lateral intake at position 115 degree was studied by Montaseri et al. [16]. The results show that the width of dividing stream surface in upper layers is greater than the layers close to the bed and the maximum width occurs below the water surface. Also, it was found that the maximum strength of secondary flow occurs at section 45 degrees of the bend. An experimental and numerical investigation of the flow characteristics in a 90°, sharp edged, rectangular open channel junction carried out by Omidbeigi et al. [17]. The comparative results indicated that the distributions of modified bed shear stresses are satisfactorily reproduced by experimental calculation. Flow structures with diversion angles of 90°, 45° and 30° were studied by Yang et al. [18]. To get better flow pattern, a diversion angle of within 30°-45° was recommended. The hydrodynamic behavior of the approaching flow and the amount of sediment entering to the right angle lateral intake in a diversion dam were investigated by Esmaili Varaki et al. [19]. Analysis of the sedimentation data showed that the sediment entered the intake by tornado-like vortex and the amount of sediment entering the intake increased with increasing intake discharge. Also, Esmaili Varaki et al. [20] have shown that in the straight canal, the intake with a diversion angle of 110 degrees has the least amount of sediment rate entering to

the intake and the width of dividing stream surface at the bottom decreases as the diversion angle increases.

As mentioned before, in channels with rectangular section, the stream tube width at the bed is more than its width at the surface. Neary and Odgaard [9] performed an experimental investigation of the flow structure at a 90 degree angle from a rectangular channel. They proposed relationships (1) and (2) for stream tube dimensions in both smooth and roughened bed, respectively (Fig.1):

$$\frac{B_s}{W_1} = 0.6 \frac{B_b}{W_1} \tag{1}$$

$$\frac{B_s}{W_1} = 0.46 \frac{B_b}{W_1} \tag{2}$$

B_s , B_b and W_1 are the stream tube width at near surface, near bed and the width of main channel, respectively. Raudkivi [21] has demonstrated relations (3) and (4) for stream tube widths using his study results, in which q_D and q are the lateral and main channel discharges, respectively. As expected, by increasing discharge ratio, the width of stream tube increases.

$$\frac{B_s}{W_2} = a_s \frac{q_D}{q} \dots\dots\dots 0.73 \leq a_s \leq 0.89 \tag{3}$$

$$\frac{B_b}{W_2} = a_b + b_b \frac{q_D}{q} \dots\dots\dots 0.37 \leq a_b \leq 0.45, 1.08 \leq b_b \leq 1.25 \tag{4}$$

Although many researches have been done on the flow pattern at lateral intakes, most of them are directed towards the intakes installed at rectangular channels, and to the knowledge of the authors, none of them have yet been carried out on stream tube dimensions and secondary current strength using experimental and mathematical models into the intakes installed at a trapezoidal channel. So, in the present research the case is treated with the 30 degree water intake installed at a trapezoidal channel.

2. MATERIALS AND METHOD

a) Experimental model

The experimental model for this study was constructed in the hydraulic laboratory of Shahid Chamran University, Ahwaz, Iran. The plan view of the experimental model is shown in Fig. 2.

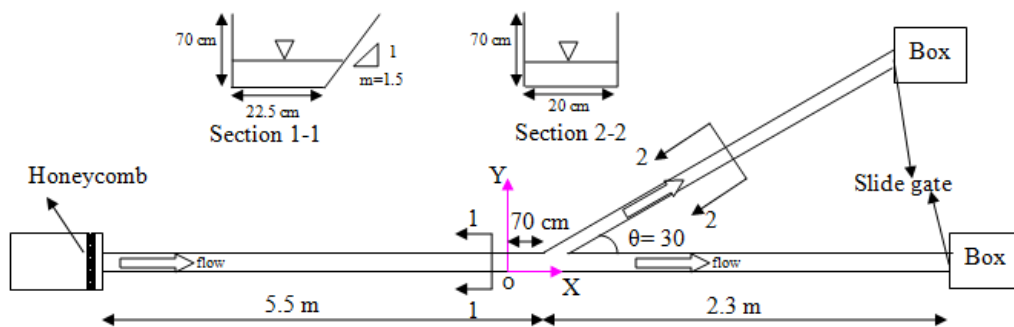


Fig. 2. Plan view of the experimental set-up for this study

The main channel and lateral glassed wall channel were 8 m and 5 m in length and 22.5 cm and 20 cm in width, respectively. The main and branch channel section were trapezoidal and rectangular respectively. The bank slope of trapezoidal section was set at 1.5:1 ($m=1.5$). The depths of both channels were 70 cm. The branch channel was set at a distance of 5.5 m from the entrance of the channel to ensure the fully developed flow has been established. The discharge was supplied from underground resource by a pump. To adjust the discharge as well as the water depth in the channels, two sluice gates are installed at their ends. To assure the flow expansion as well as low turbulence, a honeycomb was set up at the entrances of the main channel. The discharges from the main and branch channels were measured by means of two V-shaped weirs of 56 and 90 degree, respectively. The water depths in the main channel, upstream of the intake, were kept constant in all tests equal to 25 cm. Tests were, however, conducted for different approaching Froude numbers (0.25, 0.30, 0.35, 0.40 and 0.45) which were achieved by means of different flow discharge.

To perform a test, first of all, the discharge of the main channel for the corresponding depth and Froud Number was calculated, then establishing this discharge in the main channel where both downstream gates were completely opened. After the desired flow discharge was achieved and was assured to be uniform, the diversion flow ratio was measured using the V-shaped weirs. Then the downstream gates were closed up to the extent that both the diversion flow ratio and the desired flow depth were safeguarded. An Acoustic Doppler Velocimeter (ADV) was used to measure the 3D flow velocities components. The velocity measurements were performed at near the bed, 9 cm and 18 cm distances above the bed; the measurements were taken at each sampling location for 60 seconds at a sampling rate of 65 HZ. The coordinate origin (o in Fig. 2) that is in 70cm intake upstream was used for measuring. The measurements for a given flow condition lasted for 12 hours.

b) SSIIM2 model

SSIIM2 is an abbreviation for Sediment Simulation In Intakes with Multiblock Option, that is used in river, environmental, hydraulic and sedimentation engineering. The equations of Navier-Stokes that are 3D, are being used in turbulent flows to obtain the water velocity. These equations are as follows for flows with constant and non-compressible density.

$$\frac{\partial U_i}{\partial t} + U_j \frac{\partial U_i}{\partial x_j} = \frac{1}{\rho} \frac{\partial}{\partial x_j} \left(-P \delta_{ij} - \rho \overline{U_i U_j} \right) \quad (5)$$

U is flow velocity, P , pressure and δ_{ij} , kronecker delta. The first term on the left side of equation is transient term. The next term is the convective term. The first term in the right side is pressure term and the second one is Reynolds stress term. To calculate this term, a turbulence model is required. An implicit solver is used here. The SIMPLE method is the default method used for pressure- correction.

The eddy-viscosity concept is introduced with the Boussinesq approximation to model the Reynolds stress term:

$$-\overline{U_i U_j} = \nu_T \left(\frac{\partial U_j}{\partial x_i} + \frac{\partial U_i}{\partial x_j} \right) + \frac{2}{3} k \delta \quad (6)$$

The first term in right side is diffusive term in the Navier- Stokes equation. The second term is often neglected and the third one is incorporated into the pressure and is usually very small. The velocity gradient toward the wall has often steep slope. In SSIIM2 model, the default wall law is used. It is an empirical formula for rough walls:

$$\frac{U}{u_*} = \frac{1}{\kappa} \text{Ln} \left(\frac{30y}{k_s} \right) \quad (7)$$

u_* is shear velocity, k , Fan Karman coefficient (equals to 0.4) , y , distance from the wall and k_s , roughness equals to particle diameter in the bed. The $k - \varepsilon$, $k - \omega$ and RNG turbulence models can be used for this model. In this study, $k - \varepsilon$ along with RNG was utilized for model.

For inflow velocities, the Dirichlet boundary conditions and at outflow, the default zero gradient conditions were used. Due to complex 3D flows in intakes, firstly the model was run for flow conditions which were used in the experimental tests. The stream tube dimensions calculated from both experimental and SSIIM2 models were compared and the model was calibrated in such a way that the predicted and measured stream tube dimensions have a reasonable conformity. Parameters such as flexibility coefficients, time steps and turbulence model were used for model calibration. In this study, hexahedral elements of different sizes were used. The elements sizes were 1.25×0.25 cm and 2.5×0.25 cm at 10, 20, ..., 100 percentage water depth. The time step was 1second for model execution. The model meshing is shown in Fig. 3. Degree of Correlation (R^2), Root Mean Square (RMSE) and Error Percent (RE) are shown in Table1. The results comparing the profile velocity show SSIIM2 model reasonable ability in stimulating the intake flow conditions. Using the calibrated coefficients and parameters, the model was executed for different flow conditions.

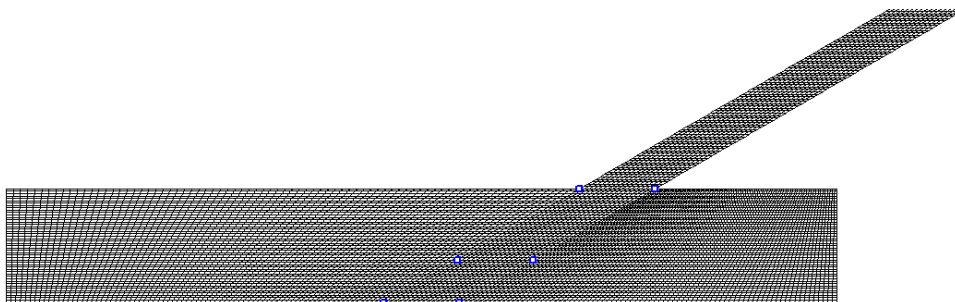


Fig. 3. Using mesh in this study

Table 1. Degree of Correlation (R^2), Root Mean Square (RMSE) and Error Percent (RE) between the width of dividing stream in numerical and experimental tests

	Testing	Verifying
R^2	0.84	0.84
RMSE	0.013	0.015
RE	12.16	11.58

As an example, Fig. 4 shows the streamlines at near, 9cm and 18 cm above the bed when the Froude number and the diversion flow ratio are equal to 0.25 and 0.3 respectively. The stream tube width (B) at each elevation from the bed is defined as the horizontal distance from the main channel bank to the last stream line of stream tube, or the line which ends at the stagnation point near the corner of downstream junction of the intake (Fig. 5).

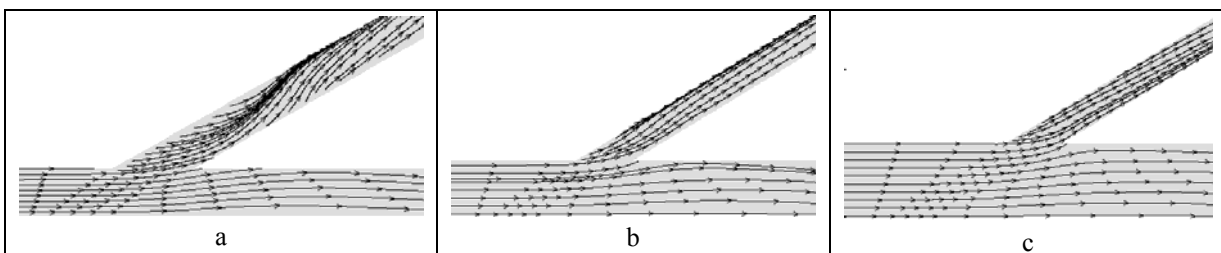


Fig. 4. The streamlines at a) near the bed b) the distance 9 cm from the bed and c) the distance 18 cm from the bed

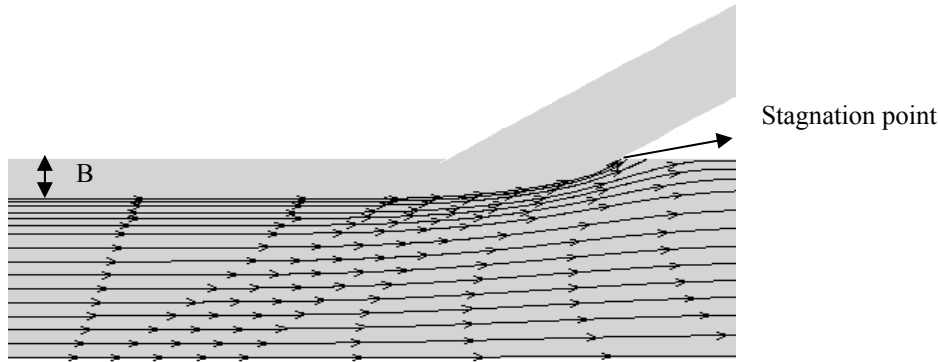


Fig. 5. The stream tube width at distance 18 cm from the bed

3. DIMENSION ANALYSIS

Since the main goal of this paper is to develop relations for predicting the stream tube dimensions, in this section a general relation is developed based on the dimensional analysis. To do so, first the most important variables are defined as: the flow discharge at the upstream of the main channel (Q_u), the secondary current strength (δ), the hydraulic depth at the upstream of the main channel (D_u), the upstream flow depth (d_u), the water density (ρ), the gravitational acceleration (g), the kinematic viscosity (ν), the mean velocity in main channel (U_1), the mean velocity in the intake (U_2), the intake angle (θ), the stream tube width (B), the stream width at a certain elevation from the bed (T), the intake width (W), the distance from the coordinate origin (Y) and the bank side slope (m). Applying the Buckingham method, the dimensionless equation may be written as follows:

$$f\left(\frac{B}{T}, \frac{U_2}{U_1}, \frac{Y}{W}, \frac{z}{d_u}, Fr, \frac{\delta}{U_1}, Q_r, \theta, m\right) = 0 \tag{8}$$

where, Fr_u is the Froud Number at the upstream of the main channel.

4. RESULTS AND DISCUSSION

Table 2 shows the range of variables for the experimental and SSIM2 model tests.

Table 2. Flow conditions in this study

m	Fr	Q_r	d_u	Method used	
				Experiment	SSIM2 Model
1.5	0.25	0.312	0.25	√	√
	0.3	0.297	0.25	√	√
	0.35	0.258	0.25	√	√
	0.4	0.3	0.25	√	√
	0.45	0.27	0.25	√	√
	0.25	0.1, 0.2, 0.3, 0.4, 0.5, 0.6	0.1, 0.2, 0.25	--	√
	0.3	0.1, 0.2, 0.3, 0.4, 0.5, 0.6	0.1, 0.2, 0.25	--	√
	0.35	0.1, 0.2, 0.3, 0.4, 0.5, 0.6	0.1, 0.2, 0.25	--	√
	0.4	0.1, 0.2, 0.3, 0.4, 0.5, 0.6	0.1, 0.2, 0.25	--	√
	0.45	0.1, 0.2, 0.3, 0.4, 0.5, 0.6	0.1, 0.2, 0.25	--	√
0	0.3	0.1, 0.2, 0.3, 0.4, 0.5, 0.6	0.25	--	√

a) Intake from rectangular canal

Firstly, the stream tube dimensions were studied for the cases of intake installed at a rectangular channel ($m=0$). Figure 6 shows the DSS boundary lines for different flow discharge ratio.

According to Fig. 6, by increasing the discharge ratio, the stream tube width at all elevations from the bed increases too. As it is clear the DSS width at the bed is much larger than in the water surface. From this figure the values of DSS width at the bottom (B_b), half of flow depth (B_m) and at the water surface (B_s) were determined. These values were normalized by T_b , T_m and T_s which are the flow width at the bottom, half of flow depth and water surface, respectively. Then the normalized B_b and B_s were plotted versus flow discharge, the results of which are shown in Fig. 7.

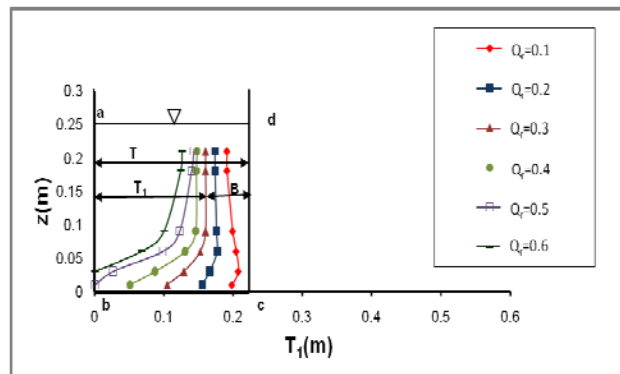


Fig. 6. DSS boundary lines for different flow conditions

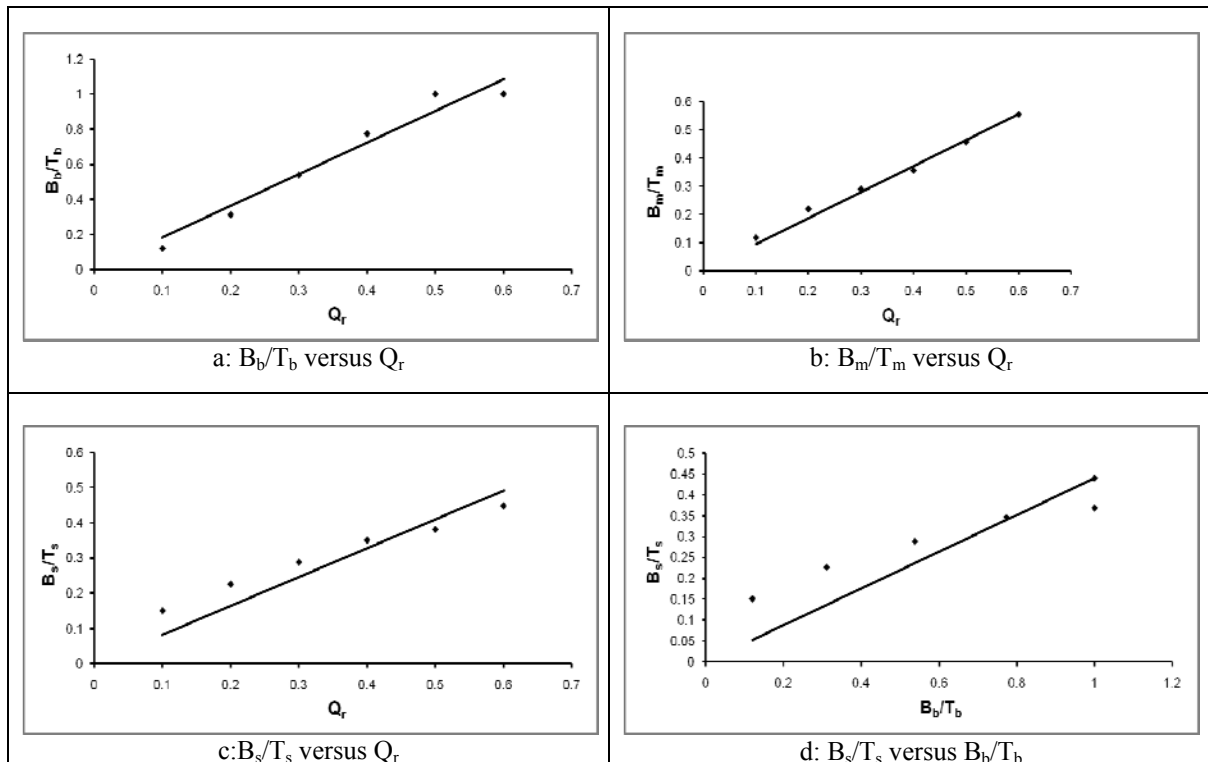


Fig. 7. Variation of normalized stream tube width at different elevation from the bed versus flow discharge at intake from rectangular canal.

Fig. 7a, 7b and 7c show that, as the flow diversion ratio increases, the DSS width increases. So, when the discharge ratio grows, more excessive discharge is provided from the bed than from the surface, consequently, when the main channel flow contains sediments, much of it is delivered into the intake; this

is because sediment concentration is much higher at the bottom than at the surface. The best lines fitted for data shown on Fig.7a, 7b and 7c were determined to be as follows:

$$\frac{B_b}{T_b} = 1.92Q_r - 0.05 \dots R^2 = 0.97 \dots Q_r, B_b > 0 \tag{9}$$

$$\frac{B_m}{T_m} = 0.85Q_r + 0.03 \dots R^2 = 0.99 \dots Q_r, B_m > 0 \tag{10}$$

$$\frac{B_s}{T_s} = 0.57Q_r + 0.11 \dots R^2 = 0.99 \dots Q_r, B_s > 0 \tag{11}$$

To correlate the DSS width at the surface to the bed, Fig.7d was plotted and the best line fitted was found to be in the form of Eq. (12). The line slope is equal to 0.28, although it is equal to 0.46 for 90 degree water intake resulting from lines different set intercept.

$$\frac{B_s}{T_s} = 0.28 \frac{B_b}{T_b} + 0.13 \dots R^2 = 0.95 \dots B_b, B_s > 0 \tag{12}$$

b) Intake from trapezoidal canal

The same procedure that was described for rectangular canal was applied for the case of intake from trapezoidal canal. The DSS was determined from each test and was plotted versus flow discharge ratio. For example, Fig. 8 shows the results for flow depth of 25cm and Froude number equal to 0.3.

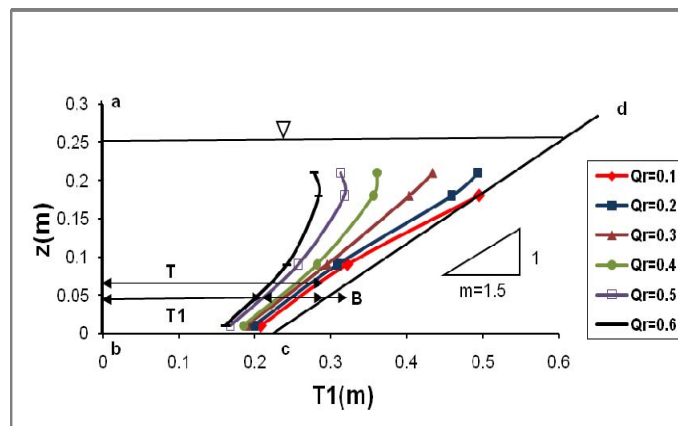


Fig. 8. DSS boundary lines at the trapezoidal canal and flow depth 25cm

It is clear from Fig. 8 that the DSS width at the surface, in contrast to the rectangular one, is larger than its width at the bed. The DSS width at the bottom, on the other hand, was found to be almost the same as the case of rectangular and does not vary significantly when the flow discharge ratio increases. The DSS width at the surface, however, is much larger than in the case of rectangular canal and increases as the flow discharge ratio increases. This is because the flow velocity at the bottom of two canals is affected by the bed roughness and remains almost equal. The flow velocity at the surface, however, is not the same for the two canals. For the case of trapezoidal canal the effect of side wall is different than for the rectangular canal. In trapezoidal section, it is found that as the flow diversion ratio increases, the stream tube width (B) increases from the bed to the water surface. The relations between diversion flow ratio (Q_r) and stream tube width in the bed (B_b), half of flow depth (B_m) and near the water surface (B_s) for water depth 10, 20 and 25 cm are shown follows:

$d_u = 10\text{cm}$

$$\frac{B_b}{T_b} = 1.113Q_r + 0.03 \dots R^2 = 0.99 \dots Q_r, B_b > 0 \tag{13}$$

$$\frac{B_m}{T_m} = 0.823Q_r + 0.01 \dots R^2 = 0.99 \dots Q_r, B_m > 0 \tag{14}$$

$$\frac{B_s}{T_s} = 0.87Q_r \dots R^2 = 0.97 \dots Q_r, B_s > 0 \tag{15}$$

$$\frac{B_s}{T_s} = 0.77 \frac{B_b}{T_b} - 0.03 \dots R^2 = 0.99 \dots B_b, B_s > 0 \tag{16}$$

$d_u = 20\text{cm}$

$$\frac{B_b}{T_b} = 0.57Q_r + 0.08 \dots R^2 = 0.96 \dots Q_r, B_b > 0 \tag{17}$$

$$\frac{B_m}{T_m} = 0.55Q_r + 0.04 \dots R^2 = 0.99 \dots Q_r, B_m > 0 \tag{18}$$

$$\frac{B_s}{T_s} = 1.02Q_r - 0.09 \dots R^2 = 0.99 \dots Q_r, B_s > 0 \tag{19}$$

$$\frac{B_s}{T_s} = 1.70 \frac{B_b}{T_b} - 0.21 \dots R^2 = 0.94 \dots B_b, B_s > 0 \tag{20}$$

$d_u = 25\text{cm}$

$$\frac{B_b}{T_b} = 0.44Q_r + 0.09 \dots R^2 = 0.94 \dots Q_r, B_b > 0 \tag{21}$$

$$\frac{B_m}{T_m} = 0.45Q_r + 0.06 \dots R^2 = 0.97 \dots Q_r, B_m > 0 \tag{22}$$

$$\frac{B_s}{T_s} = 1.03Q_r - 0.10 \dots R^2 = 0.99 \dots Q_r, B_s > 0 \tag{23}$$

$$\frac{B_s}{T_s} = 2.20 \frac{B_b}{T_b} - 0.27 \dots R^2 = 0.92 \dots B_b, B_s > 0 \tag{24}$$

The analysis of the results show that for the flow depth of 10 cm depth, while increasing the discharge ratio, the stream tube width at the bed and surface increases uniformly. For the case of trapezoidal channel in contrast to rectangular, as the flow diversion ratio increases, the stream tube width increases in the surface more vigorously, especially for flow depth of 20 and 25 cm depth (the lines slope in equations 15, 19 and 23 is more steep than equation 11). So, when the discharge ratio grows, more excessive discharge is provided from the surface than from the bed, consequently, in case where the main channel flow contains sediments, much less of them delivery into the intake. The results show that for the same flow conditions, the surface stream tube width for intake from trapezoidal channel can increase twice

as the same width for intake from rectangular channel. The bottom width of stream tube, on the other hand, is decrease to about 70 percent for intake from trapezoidal channel in comparison to intake from rectangular channel. By careful consideration of the above equations it can be seen that for the same flow discharge ratio, the bottom stream tube width is much lower when the flow depth is higher. For example, for $Q_r=0.3$, the bottom stream tube (B_b) is equal to $0.59T_b$, $0.37T_b$ and $0.31T_b$ for flow depth of 10, 20 and 25cm respectively. This means that in canal with higher flow depth, the major portion of flow discharge to the intake is provided from the upper layers.

c) Secondary current

As it was mentioned before, a secondary vortex is created spiral near the outside bank of the diversion channel due to the velocity non-vertical distribution and high velocity at the water surface than at the bed. Spiral movement of this current will cause the entry of sediment into the intake. The strength of this vortex which is an indication of sediment entry to the intake, in each section of the intake depends on the transverse velocity difference at the water surface and at the bed. So, the secondary current strength can be defined as (Neary and Odgaard [9]):

$$\delta = U_s - U_b \quad (25)$$

δ is the secondary current strength; U_s and U_b are transverse velocity at the water surface and at the bed of the intake, respectively. In this study, when the main channel bank was vertical, the secondary current was studied in different diversion discharge ratios for the water depth of 25 cm and Froude number equal to 0.3. For the trapezoidal canal, the secondary current was studied for different flow conditions in which the flow depth was equal to 10, 20 and 25 cm for Froude number equal to 0.3. δ was calculated from Eq. 25 and normalized by U_1 , the approaching average flow velocity and plotted versus Y/W or the ratio of the distance from origin coordinate in Y direction to the channel branch width. The result for the case of rectangular channel is shown in Fig. 9.

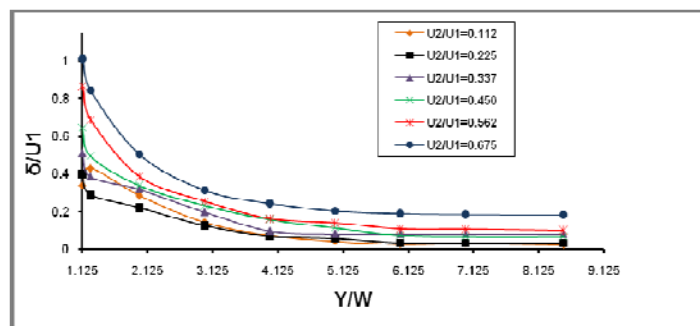


Fig. 9. δ / U_1 for the case of rectangular channel

Figure 9 shows that the secondary current strength for the rectangular channel decays as it proceeds downstream, primarily due to flow viscosity. The maximum secondary current strength occurs in the intake entrance and $\frac{Y}{W} = 1.125$. At this point the δ / U_1 ratio depends on the flow discharge ratio or U_2 / U_1 according to the following relation:

$$\frac{\delta}{U_1} = 1.14 \left(\frac{U_2}{U_1} \right)^{0.62} \dots R^2 = 0.92 \dots d_u = 25 \text{ cm} \quad (26)$$

For the case of trapezoidal channel, Fig. 10 was plotted. From Fig.10 can be seen that when the upstream water depth is 10cm, the maximum secondary current strength is at $\frac{Y}{W} = 1.125$ and will

decrease while proceeding downstream. For flow depth of 20 and 25cm, the secondary current starts from $\frac{Y}{W} = 2.5$ and $\frac{Y}{W} = 3$, respectively and decreases along the intake. The relation between $\frac{U_2}{U_1}$ and $\frac{\delta}{U_1}$ ratios for different water depth at a section with maximum strength of secondary current can be obtained to be as follows:

$$\frac{\delta}{U_1} = 0.26 \left(\frac{U_2}{U_1} \right)^{1.73} \dots\dots R^2 = 0.99 \dots d_u = 10cm \tag{27}$$

$$\frac{\delta}{U_1} = 0.3 \left(\frac{U_2}{U_1} \right)^{1.48} \dots\dots R^2 = 0.99 \dots d_u = 20cm \tag{28}$$

$$\frac{\delta}{U_1} = 0.33 \left(\frac{U_2}{U_1} \right)^{1.29} \dots\dots R^2 = 0.96 \dots d_u = 25cm \tag{29}$$

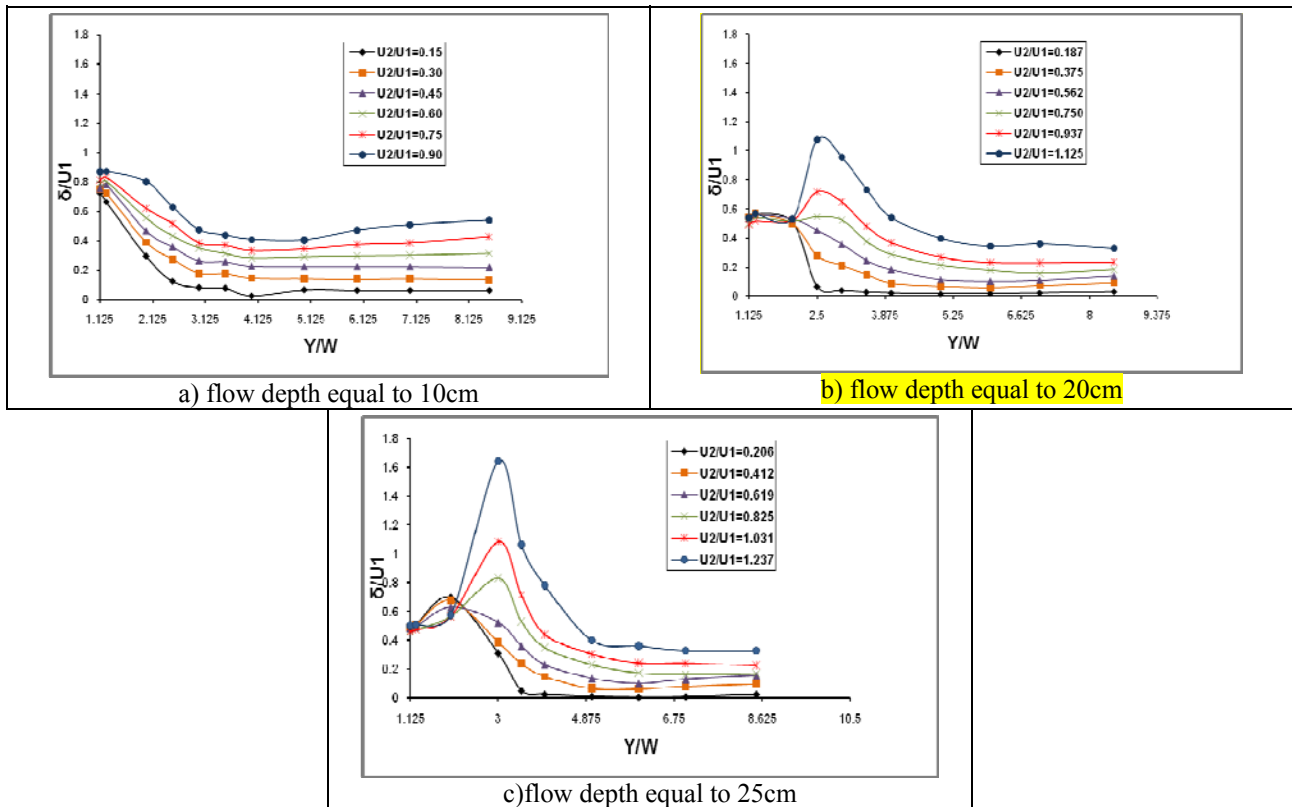


Fig. 10. $\frac{\delta}{U_1}$ for the case of trapezoidal channel

It should be noted that, for different diversion discharge ratios, the Froude number in the main channel upstream was constant and was equal to 0.3. For flow depth of 10 cm, for different $\frac{U_2}{U_1}$ ratios, $\frac{\delta}{U_1}$ ratio decay from the intake entrance toward the end of intake, for flow depth of 20 cm and 25 cm, $\frac{\delta}{U_1}$ ratio at intake entrance first increased to its maximum, then decayed toward the end of intake. So, there is a turnoff point between 10 cm water depth and the two in which afterwards, the secondary current

forms completely. As maintained by Raudkivi [21], the secondary current strength declines along with the increase of the roughness ratio ($\frac{k_s}{D_u}$). k_s and D_u are the bed roughness and the hydraulic depth at the upstream of the main channel, respectively. The roughness ratio increases along with the decrease of water depth. So, the roughness ratio corresponding to the water depth 10 cm is high ($\frac{k_s}{D_u} = 18.75E-6$) therefore the strength of secondary current decreases at the entrance, followed by decrease of the sediment entry.

Figure 11 shows the comparison between maximum secondary current strength for water intake installed from rectangular and trapezoidal main channel for flow depth of 25 cm. It is clear that, for a constant $\frac{U_2}{U_1}$ ratio, the $\frac{\delta}{U_1}$ ratio at water intake installed at a trapezoidal main channel is less than the rectangular ones.

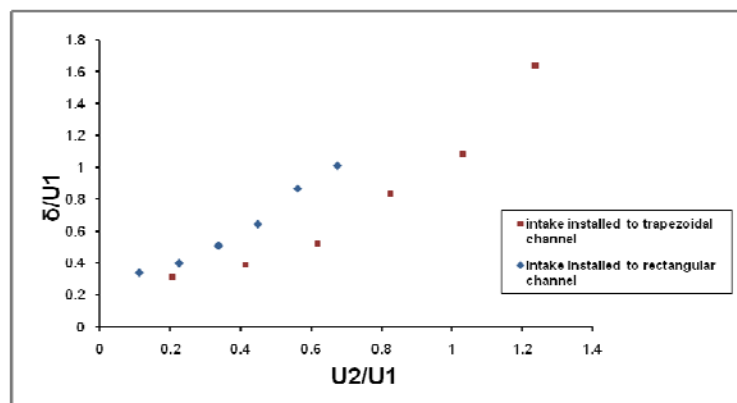


Fig. 11. The maximum secondary current strength at water intake installed to rectangular and trapezoidal channel

5. CONCLUSION

In this study, the stream tube width and the secondary current strength were investigated for 30 degree angle intake installed at the bank of both rectangular and trapezoidal channel. The experimental tests were performed to get enough data to calibrate the numerical (SSIIM2) models. More data was obtained from the model. From the analysis of all data it was found that the dividing stream width at different elevation from the bed depends directly on the diversion flow ratio. Different relations were presented for prediction of stream tube dimensions for intake installed at trapezoidal channel. Comparison of these equations with the case of intake from rectangular channel found that by inclining the channel bank, the surface stream tube width increases (up to 200%) while the bottom stream tube width decreases (as much as 70%). Also, the secondary current strength, which is an indication of sediment entry to the intake, was calculated for all tests. The results show that it is directly proportional to the flow diversion ratio and for the same flow conditions it has a much lower value for channel with inclined banks than with vertical walls. The above results, reduction of bottom stream tube width and reduction of secondary current strength as the channel banks inclined, resulted in reduction of less suspended sediment entry to the intake due to the fact that sediment concentration is much higher at the bottom.

Acknowledgement: This study was supported financially from the applied research department of Iranian Water Resources Management Company under grant No.3-88039RIV.

REFERENCES

1. Taylor, E. (1944). Flow characteristics at rectangular open channel junctions. *Trans., ASCE*, Vol. 109, pp. 893-912.
2. Thomson, L. M. (1949). *Theoretical hydrodynamics*. 2nd ed., MacMillan, London.
3. Tanaka, K. (1957). The improvement of the inlet of the Power Canal. *Transactions of the Seventh General Meeting of I.A.H.R.*, Vol. 1, No. 17.
4. Murota, A. (1958). On the flow characteristics of a channel with a distributory. *Technology Reports of the Osaka University*, Vol. 6, No. 198.
5. Grace, J. L. & Priest, M. S. (1958). Division of flow in open channel junctions. *Engineering experimental Station, Alabama, Polytechnic Institute, Auburn, Ala. Bulletin*, No. 31
6. Law, S. W. & Reynolds, A. J. (1966). Dividing flow in an open channel. *J. Hydr. Div.*, Vol. 92, No. 2, pp. 4730-4736.
7. Hager, W. H. (1984). An approximate treatment of flow in branches and bends. *Proc., Instn. Mech, Engrs.*, Vol. 198C, No. 4, pp. 63-69.
8. Hager, W. H. (1992). Discussion of 'Dividing flow in open channels' by Ramamurthy, A.S, Tran, D.M. & Carballada, L.B. *J. Hydraul.Eng.*, Vol. 118, No. 4, pp. 634-637.
9. Neary, V. S. & Odgaard A. J. (1993). Three-dimensional flow structure at open-channel diversions. *Journal of Hydraulic Engineering ASCE*, Vol. 119, No. 11, pp. 1223-1230.
10. Neary, V. S., Sotiropoulos, F. & Odgaard, A. J. (1999). Threedimensional numerical model of lateral-intake inflows. *J. Hydraul. Eng.*, Vol. 125, No. 2, pp. 126-140.
11. Barkdoll, B. D. (1999). Sediment control at lateral diversions: Limits and enhancements to vane use. *Journal of Hydraulic Engineering ASCE*, Vol. 125, No. 8, pp. 826-870.
12. Weber, L. J., Schumate, E. D. & Mawer, N. (2001). Experiments on flow at a 90° open-channel junction. *J. Hydraul. Eng.*, Vol. 127, No. 5. pp. 340-350.
13. Huang, J., Weber L. J. & Lai, Y. G. (2002). Three-dimensional numerical study of flows in open-channel junctions. *J. Hydraul. Eng.*, Vol. 128, No. 3, pp. 268-280.
14. Mohammadi, M. (2005). The initiation of sediment motion in fixed bed channels. *Iranian Journal of Science & Technology, Transaction B, Engineering*, Vol. 29, No. B3, pp. 365-372.
15. Ramamurthy, A. S., Junying, Q. U. & Diep, V. O. (2007). Numerical and Experimental Study of Dividing open-channel flows. *Journal of Hydraulic Engineering ASCE*, Vol. 133, No. 10, pp. 1135-1144.
16. Montaseri, H., Ghodsian, M., Shafieefar, M., Salehi Neyshabouri, S. A. A. & Dehghani, A. A. (2008). Experimental investigation of 3D flow field and scouring in a U shape rectangular channel with a lateral intake. *J. Agric. Sci. Natur. Resour.*, Vol. 15, No. 2.
17. Omidbeigi, M. A., Ayyoubzadeh, S. A. & Safarzadeh, A. (2009). Experimental and numerical investigations of velocity field and bed shear stresses in a channel with lateral intake. *33rd IAHR Congress, Vancouver, Canada*, pp. 1284-1291.
18. Yang, F., Chen, H. & Guo, J. (2009). Study on "diversion angle effect" of lateral intake flow. *33th IAHR Congress, Vancouver, Canada*, pp. 4509-4516.
19. Esmaili Varaki, M., Farhoudi, J. & Walker, D. (2009). Investigation of flow at a right -angled lateral intake. *ICE, J. Water Management*, Vol. 162, No. 6, pp. 379-388.
20. Esmaili Varaki, M., Farhoudi, J. & Walker, D. (2011). Study of flow structure and sediment entry to a lateral intake. *ICE, J. Water Management*, Vol. 167, No. 7, pp. 346-360.
21. Raudkivi, A. J. (1993). Sedimentation, exclusion and removal of sediment from diverted water. *IAHR. AIRH. Hydraulic Structures*.